View Journal

# PCCP

## Accepted Manuscript

This article can be cited before page numbers have been issued, to do this please use: C. Campanella, E. Lopez-Fontal, S. Tomas and L. Milanesi, *Phys. Chem. Chem. Phys.*, 2017, DOI: 10.1039/C7CP01127J.




ROYAL SOCIETY OF CHEMISTRY

rsc.li/pccp

View Article Online
DOI: 10.1039/C7CP01127J

Journal Name

ARTICLE

Received 00th January 20xx,

Accepted 00th January 20xx

DOI: 10.1039/x0xx00000x

www.rsc.org/



# Modulation of the cooperativity in the assembly of multistranded supramolecular polymers

Cristiana Campanella,[a] Elkin Lopez-Fontal,[b] Salvador Tomas *,[b] and Lilia Milanesi*,[a]

It is highly desirable that supramolecular polymers self-assemble following small changes in the environment. The degree of responsiveness depends on the degree of cooperativity at play during the assembly. Undertanding how to modulate and quantify cooperativity is therefore highly desirable for the study and design of responsive polymers. Here we show that the cooperative assembly of a porphyrin-based, double-stranded polymer is triggered by changes in building blocks and in salt concentration. We develop a model that accounts for this responsiveness by assuming the binding of the salt countercations to the double-stranded polymer. Using our assembly model we generate plots that show the increase in concentration of polymer versus the normalized concentration of monomer. These plots are ideally suited to appreciate changes in cooperativity, and show that, for our system, these changes are consistent with the increase in polymer length observed experimentally. Unexpectedly, we find that polymer stability increases when cooperativity decreases. We attribute this behaviour to the fact that increasing salt concentration stabilizes the overall polymer more than the nucleus. In other words, the cooperativity factor $\alpha$, defined as the ratio between the growth constant $K_g$ and the nucleation constant $K_n$ decreases as the overall stability of the polymer increases. Using our model to simulate the data, we generate cooperativity plots to explore changes in cooperativity for multistranded polymers. We find that, for the same pairwise association constants, the cooperativity sharply increases with the number of strands in the polymer. We attribute this dependence to the fact that the larger the number of strands, the larger is the nucleus necessary to trigger polymer growth. We show therefore that the cooperativty factor $\alpha$ does not properly account for the cooperativity behaviour of multistranded polymers, or any supramolecular polymer with a nucleus composed of more than 2 building blocks, and propose the use of the corrected cooperativity factor $\alpha_m$. Finally, we show that multistranded polymers display highly cooperative polymerisation with pairwise association constants as low as 10 $M^{-1}$ between the building blocks, which should simplify the design of responsive supramolecular polymers.

## Introduction

Many molecules assemble into long 1D structures by means of weak intermolecular interactions, leading to supramolecular polymers.[1-3] On account of the weak intermolecular interactions that hold the building blocks together, these polymers are dynamic structures' i.e., capable of self-organise into large scale assemblies in response to specific stimuli.[4,5] This process plays a key role in the function of biological systems. Examples are cell division and motility which are regulated by dynamic assembly of microtubules and actin filaments, respectively.[6-8] Some small synthetic molecules also undergo supramolecular polymerization to yield hydrogels that assemble and disassemble in response to external stimuli,[9,10] and are being developed for applications in controlled drug delivery[11,12] and tissue engineering.[13-15] Synthetic supramolecular polymers are also being exploited in nanofabrication, for the development of nanowires[16-19] or as components of artificial molecular machines.[20] For such applications, what is required are molecules that, like their biological counterparts, polymerize and de-polymerize in response to small environmental changes. This behaviour requires that the polymerization is cooperative. As opposite to isodesmic polymerization, that leads to the steady growth as the monomer concentration increases, cooperative polymerization results in a nucleation-growth type of mechanism, where polymers form suddenly upon reaching the nucleation concentration.[21-23] For these polymers, small environmental changes (including changes in pH, temperature or salt concentration[24-26]) may modify the nucleation concentration (*NC*) switching on or off the polymerization. Porphyrin-containing polymers are of particular interest for

[a] School of Biological and Chemical Sciences, Queen Mary University of London, Mile End Road, London E1 4NS, UK.
[b] Institute of Structural and Molecular Biology and Department of Biological Sciences, School of Science, Birkbeck University of London, Malet Street, London WC1E 7HX, UK.

† Footnotes relating to the title and/or authors should appear here.
Electronic Supplementary Information (ESI) available: Detailed derivatization of the equations and detailed procedure for fitting to the non-allosteric $Na^+$ binding model See DOI: 10.1039/x0xx00000x

View Article Online
DOI: 10.1039/C7CP01271





the development of nano-scale optical and electronic devices.[16,18,27] Their spectroscopic properties make them also ideally suited to study in detail mechanisms of supramolecular polymerization. [28-30]

We have recently described the assembly of cobalt metalloporphyrin **C** and bipyridine **B**. **C** and **B** form linear oligomers by the alternating assembly of **C** and **B** building blocks.[31] These oligomers dimerize, leading to double stranded polymers. The formation of these polymers follows a nucleation-growth mechanism, which we have described using a model that combines the isodesmic oligomerization of single stranded oligomers (characterized by the oligomerization constant $K_o$) with the dimerization of the oligomers into double stranded polymers (characterized by the lateral association constant $K_l$). Our model identifies multivalency as the root of the cooperativity leading to the formation of the polymer. However, an optimal control of the assembly (and, hence, of responsiveness) requires also an understanding of how the degree of cooperativity can be manipulated.[22] This understanding can be applied to design monomers for which polymerization can be finely controlled and ultimately a desired functionality achieved.

Here we carry out the detailed study of how the polymerization of our porphyrin-bipyridine building blocks responds to changes in salt concentration. To avoid complicating effects due to potential binding of the chlorine anion to the porphyrin metal we use sodium phosphate as the salt in all the experiments. We develop a model that allow us to fully account for the spectroscopic data and to show that changes in the salt concentration affect the lateral association constant of the oligomers (i.e. $K_l$) but have no effect on the oligomerization constant of the single stranded oligomers (i.e. $K_o$). This is explained in terms of the salt countercations binding to the double stranded oligomers but not to the single stranded oligomer. We find that increasing $K_l$ leads to an increase in the stability of the polymer, but reduces the degree of cooperativity in the polymerization. This trend is opposite to the behaviour observed in other systems that display a dependence of assembly cooperativity with salt concentration.[26] We show that this apparent contradiction is due to the fact that an increase in $K_l$ stabilizes the nucleus to a larger extent than it stabilizes the overall polymer. We also show that the degree of cooperativity strongly depends on the number of building blocks required for the assembly of the nucleus. As a consequence, polymers composed of 5 or more strands can show a high degree of cooperativity even with very low values of $K_o$ and $K_l$ (i.e., down to 10 $M^{-1}$).

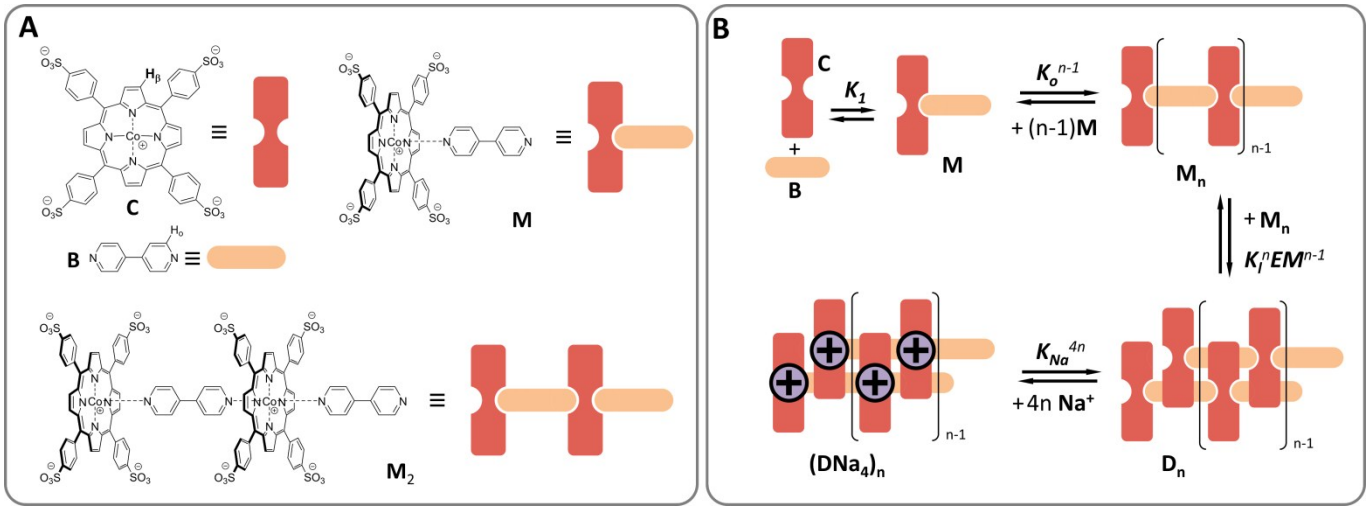


**Figure 1.** A. Chemical structure of the building blocks and their cartoon representation. B. Schematic representation of the formation of single and double stranded polymers in solutions containing equal concentrations of **C** and **B**. The binding of Na cations to the double stranded polymer is also shown.

## Results and discussion

We have recently shown[31] that cobalt metalloporphyrin **C** and bipyridine **B** form complexes of the form **CB**, with a binding constant $K_1$ of $1.14 \times 10^6$ $M^{-1}$. We call these complexes monomers **M**, that oligomerise into single stranded oligomers of the form $\mathbf{M}_n$ following an isodesmic (i.e., non-cooperative) mechanism, with oligomerization constant $K_o$ = 8400 $M^{-1}$. **M** forms also double-stranded polymers of the form $(\mathbf{M}_n)_2$, following a nucleation-growth (i.e., cooperative) mechanism (Figure 1A and 1B). The formation of $(\mathbf{M}_n)_2$ can be seen as the dimerization of linear $\mathbf{M}_n$ oligomers, with a dimerization constant $K_{nl}$. This constant can be written as a function of the dimerization constant per unit repeat, $K_l$, and the effective molarity (i.e., a measure of the local concentration of the polymer repeats within the polymer) *EM* as follows:

$$K_{nl} = K_l{}^n EM^{n-1} \qquad (1)$$

where *n* is the number of oligomer repeats in the dimerizing oligomers. With the product $K_l$ x *EM* larger than 1, near-quantitative dimerization of single stranded oligomers takes place once they reach a critical size, owing to a positive multivalence cooperativity effect. At this critical nucleation

View Article Online
DOI: 10.1039/C7CP01271J



concentration (*NC*) the double-stranded polymer experiences a sudden growth as the total concentration of monomers increases. [31]

At low salt concentration (i.e., 5 mM phosphate, pH 7.2) the *NC* of the double stranded polymer is approx. 500 μM., which means that it does not form below this concentration.[31] However, addition of salt to a sample of **C** and **B** both 10 μM results in the growth of a red-shifted Soret band, characteristic of the formation of the double stranded polymer, when the concentration of salt approaches 100 mM (Figure 2A). Similarly, increasing the concentration of buffer in a sample containing equimolar **C** and **B** 25 μM leads to the loss of the NMR signals assigned to **C**, consistent with the formation of large polymers (Figure 2B). It is reasonable to attribute these changes to an increase in the pairwise binding constants $K_o$ and $K_I$, because increasing ionic strength reduces the electrostatic repulsion between the anionic porphyrin units. $K_o$ can be written as a function of the different binding constants for the formation of **CB**, $\mathbf{C_2B}$ and $\mathbf{CB_2}$ complexes.[31] The value of these binding constants is however the same, within the error, for different buffer concentrations (i.e., 5 and 100 mM) which means that $K_o$ does not depend on the concentration of buffer.[31] This result suggests that the bi-pyridine ligand keeps the anionic porphyrin rings far apart enough to render electrostatic repulsion between them negligible within the single stranded oligomers. The distance between negative charges in the double stranded polymer is however much smaller (Figure 2C). The implication is that $K_I$ will be affected by changes in ionic strength to a greater extent than $K_o$. Specifically $K_I$ is expected to increase as the ionic strength increases because of the increase in the screening of the sulphonate negative charges provided by the salt countercations. The effect of the ionic strength on the interactions between charged species, particularly in supramolecular polymerization, can be treated using the Debye-Huckel model.[26] An alternative, convenient way to seamlessly incorporate the effect of the salt in our assembly model is to consider the binding of the countercations to the different species present. In our experiments, Porphyrin **C** is used in the tetrasodium salt form. However, given the low concentration of **C** (0.5 to 140 μM) in relation to the buffer concentration (2 to 500 mM), the contribution of the sodium cations coming from **C** to the total concentration of sodium is negligible.

For **C**, **M** and single stranded polymer $\mathbf{M}_n$ the negative charges located are far apart in the structure so that no more than one anion can interact with a countercation. For $(\mathbf{M}_n)_2$ on the other hand negative charges are brought in close proximity upon double strand formation. As a consequence, a countercation can interact simultaneously with two or more anions. In fact, a close inspection of the structure of the polymer dimer, constructed from single-crystal derived structures,[32] shows the presence of up to 4 potential binding sites for the sodium cation, in the form of cavities surrounded by up to 4 sulfonate groups for each polymer repeat (Figure 2C). It is therefore reasonable to assume that the cation binds much more strongly to these cavities than to the single stranded polymer or to other sites in the double stranded polymers. To model the effect of the salt, we thus assume that $Na^+$ binds exclusively to the double stranded polymers. For simplicity of notation, we call the repeat units within the double-stranded polymer **D**, so that $(\mathbf{M}_n)_2$ can be noted $\mathbf{D}_n$ (Figure 1B). The binding of up to 4 Na cations to the polymer repeat **D** leads to polymer repeats of the form $Na_i\mathbf{D}$, with *i* values up to 4 for full occupancy. We can assume that the affinity for $Na^+$ for each of the binding sites is intrinsically the same, that is, the binding of the $Na^+$ is non-cooperative (see Supplementary Information and Supplementary Figure 1). The relative rapid rise of polymer concentration with increasing salt concentration, as shown by the experimental data (Figure 2A inset), is consistent however with a model in which the binding of $Na^+$ is cooperative.

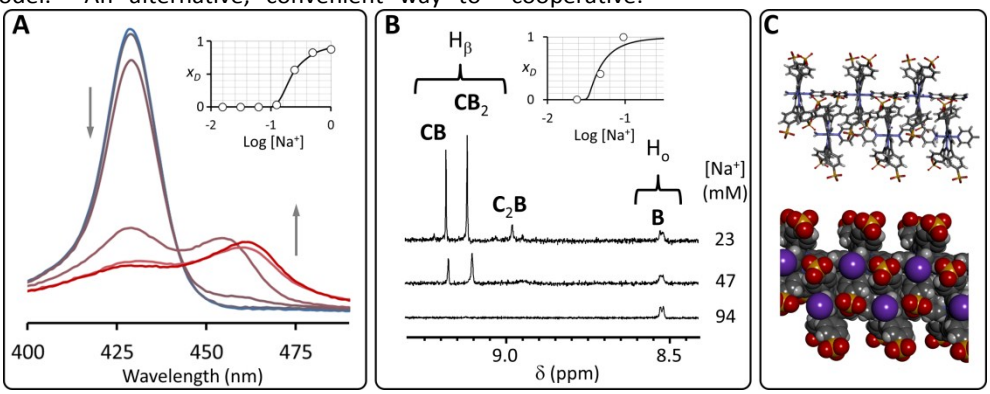


**Figure 2**. A. Changes in the Soret band region of the UV spectrum of an equimolar solution of **C** and **B** ([**C**] = 10 μM) upon increasing the concentration of buffer. The inset shows the changes in the mol fraction of double stranded polymer, $x_D$, derived from the UV data (empty circles). The continuous line is the simulated change in $x_D$ by our model for a $K_{Na}$ of 70 $M^{-1}$ (See Supplementary Information for details). B. Section of the $^1$H NMR spectrum of a mixture of **C** and **B** showing the peaks assigned to the β proton of **C** in discrete complexes and the ortho proton ($H_o$) of free **B** (see Figure 1A for the proton labelling scheme) at different concentrations of $Na^+$. The concentration of **C** was 34 μM and that of **B** 51 μM in all cases. The inset shows the changes in the mole fraction of the double stranded polymer derived from the integration of the NMR signals (empty circles). The continuous line is the changes in $x_D$ projected by our model for a $K_{Na}$ of 70 $M^{-1}$. C Molecular model of the double stranded polymer, derived from a crystal structure of the **C** and **B** complex [31,32] (top). In the bottom, the same model is shown in a CPK representation, with Na cations placed in the cavities defined by the sulfonate groups.

View Article Online
DOI: 10.1039/C7CP01127J

Journal Name

ARTICLE



A scenario can be envisaged in which potential binding sites for $Na^+$ within the polymer-dimer repeats are ill-defined prior to binding of any cation, and become fixed in position after the initial binding events take place, making subsequent events more likely (and therefore displaying larger binding affinity constants). This scenario describes a typical allosteric binding, with the binding affinity increasing as the occupancy increases. In the upper limit of cooperativity of allosteric binding, only the complex with full occupancy, that is, $Na_4\mathbf{D}$, is populated to a meaningful extent. The average binding constant for $Na^+$, $K_{Na}$, is related to the concentrations of complex and free species as follows:

$$K_{Na}{}^4 = \frac{[\mathrm{Na_4D}]}{[\mathbf{D}][\mathrm{Na}]^4} \qquad (2).$$

We can then write the lateral association constant $K_l$ as a function of the concentration of $Na^+$ as follows (see Supplementary Information for details):

$$K_l = K_{l0}(1 + K_{Na}{}^4[\mathrm{Na}]^4) \qquad (3)$$

where $K_{l0}$ is the value of lateral association constant in the absence of $Na^+$. When the concentration of both **B** and **C** are the same, the total concentration of **C**, $[\mathbf{C}]_0$, can be written as a function of free **C** as follows (see Supplementary Information for details):

$$[\mathbf{C}]_0 = [\mathbf{C}] + \frac{K_1[\mathbf{C}]^2}{(1-K_oK_1[\mathbf{C}]^2)^2} + \frac{2K_{l0}(1+K_{Na}{}^4[\mathrm{Na}]^4)K_1{}^2[\mathbf{C}]^4}{\left(1-K_{l0}(1+K_{Na}{}^4[\mathrm{Na}]^4)EM(K_oK_1[\mathbf{C}]^2)^2\right)^2} \qquad (4)$$

While the total concentration of **D** repeats, [**D**], can be written as a function of **C** and the concentration of $Na^+$ as follows:

$$[\mathbf{D}] = \frac{K_{l0}(1+K_{Na}{}^4[\mathrm{Na}]^4)K_1{}^2[\mathbf{C}]^4}{\left(1-K_{l0}(1+K_{Na}{}^4[\mathrm{Na}]^4)EM(K_oK_1[\mathbf{C}]^2)^2\right)^2} \qquad (5)$$

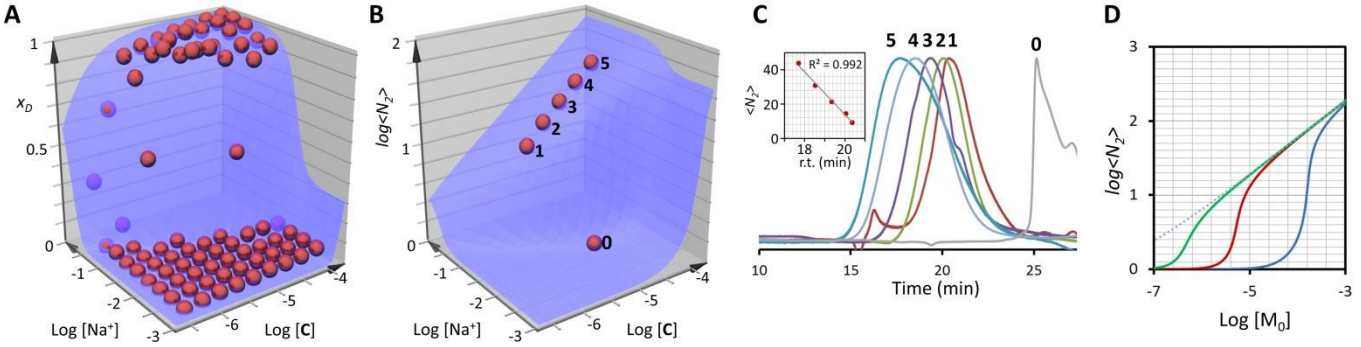


**Figure 3**. A. Changes of the mole fraction of monomer within the double stranded polymer, $x_D$, with the concentration of $Na^+$ and the total concentration of **C** (which is equal to that of **B**). The red spheres are the experimental values of $x_D$ calculated from the UV spectra (see Supplementary information for details). The blue surface is the best fit to the model described by equations 4, 5 and 6. B. Changes in the average number of repeats of the double stranded polymer, $<N_2>$, as a function of $Na^+$ and the total concentration of **C** (which is equal to that of **B**) (blue surface). The red spheres correspond to the predicted values of $<N_2>$ for the samples analysed by size exclusion chromatography (SEC) in panel C. C. SEC traces of choice samples with increasing concentration of building blocks (concentration of salt 125 mM). For reference, a trace corresponding to a sample without double stranded polymer (trace 0) is also shown. The inset shows the correlation between predicted number of repeats and the retention time of the corresponding peak. D. Changes in the average number of repeat of a double stranded polymer as a function of the total concentration of monomer for values of $K_lEM$ =5 (blue trace), 500 (red trace) and 50000 (green trace) $M^{-1}$ obtained using eq. 7 with $EM$=1 M and $K_o$ = 8400 $M^{-1}$. The dotted line represents the change in $<N_2>$ for $K_lEM = \infty$.

The double stranded polymer $\mathbf{D}_n$ is the species responsible for the red-sifted band with maxima at around 460 nm in the UV spectrum, while all the other species present (i.e., single stranded $\mathbf{M}_n$, double stranded $\mathbf{D}_n$ and free **C**) contribute to the absorbance at 430 nm (Figure 2A).[31] The mole fraction of building block **C** in in the double stranded polymer $\mathbf{D}_n$ over the concentration of total **C**, $x_D$, can be calculated from the ratio of absorbance at 460 nm over that at 430 nm, $x_A$ , as follows (see Supplementary Information for details):

$$\frac{2[\mathbf{D}]}{[\mathbf{C}]_0} = x_D = \frac{\varepsilon_{R1}x_A}{1-x_A(1+\varepsilon_{R2}-\varepsilon_{R3})} \qquad (6)$$

where $\varepsilon_{R1}$, $\varepsilon_{R2}$ and $\varepsilon_{R3}$ are appropriate ratios of extinction coefficients of **D** and that of the non-polymeric species present (see Supplementary Table 1 and Supplementary Information for details). We carried out an UV titration-dilution experiment where samples containing equimolar amounts of **C** and **B** were diluted and each of the dilutions titrated with sodium phosphate. The relevant data from the UV spectra was

used to calculate $x_D$, and these values were fitted to the model defined by equations 4, 5 and 6 (Figure 3A, inset of Figure 2A and 2B). $K_1$ (with a value of $1.14 \times 10^6$ $M^{-1}$) and $K_o$ (with a value of 8400 $M^{-1}$) had been previously determined, together with $K_l$ in buffer phosphate 5 mM (with $EM$ = 1). We can assume that at this low buffer concentration, the value of $K_l$ is $K_{l0}$ (i.e., 6.1 $M^{-1}$).[31] In the fitting, we enter these values as fixed parameter and only $K_{Na}$ is optimized. In these conditions the fitting of the model to the experimental data is very good, giving a value of $K_{Na}$ of 70 $M^{-1}$. This is a reasonable value for a receptor of $Na^+$ in water, in the same range found for some biological receptors.[33] We reiterate that the $Na^+$ binding model is a convenient way of incorporating the effect of the buffer into our model. Although the only evidence for this binding event taking place is that the size of the cavities of the polymer is large enough to accommodate one $Na^+$ (Figure 2C), both the close fitting of the data to the modified binding model and the reasonable values for $K_{Na}$ obtained suggest that our approach offers a valid description of the phenomenon under study.

Knowing $K_{Na}$, it is possible to determine the average number of repeats of the double stranded polymer , $<N_2>$, as a function of the concentration of $Na^+$ and building blocks **C** and **B**. For solutions with equal concentration of **C** and **B**, $<N_2>$ can be written as:

$$< N_2 >= \frac{1}{1-{K_o}^2 EMK_{l0}(1+{K_{Na}}^4[\mathrm{Na}]^4)(K_1[\mathbf{C}]^2)^2} \qquad (7)$$

Size exclusion chromatography performed on samples with increasing concentration of **C** and **B** yield results that are consistent with the variations predicted by equation (7): there is a jump in size around the nucleation concentration, and a subsequent smooth increase of the size of the polymer as the concentration increases (Figure 3B and 3C). The magnitude of the jump in the average number of repeats of the double stranded polymer, $<N_2>$, upon nucleation depends on the concentration of $Na^+$, and is attributed to changes in $K_l$ as the concentration of $Na^+$ is changed. This dependence is more clearly seen by plotting $<N_2>$ as a function of the changes in total concentration of monomer at constant $K_o$ but with different values of $K_l$ (with $EM$ = 1) (Figure 3D). This plot shows that the jump in the size of the polymer becomes both larger and steeper as $K_l$ decreases. Cooperativity in binding is characterized by the steep increase of the concentration of bound species when a critical concentration of the building blocks is reached. The larger the degree of cooperativity, the steeper is this increase, leading to an on/off behaviour in systems displaying very high degree of cooperativity. For this reason, the steeper increase in the jump of $<N_2>$ at lower $K_l$ suggests that the degree of cooperativity increases as $K_l$ decreases. The implications are that, in our system, the degree of cooperativity decreases as the stability of the resulting polymer increases. This behaviour is opposite to the one observed in other examples of supramolecular polymerisation modulated by the salt content. For example, Schaefer *et al.* found that the stability and degree of cooperativity both increased as the ionic strength in the medium increased.[26]

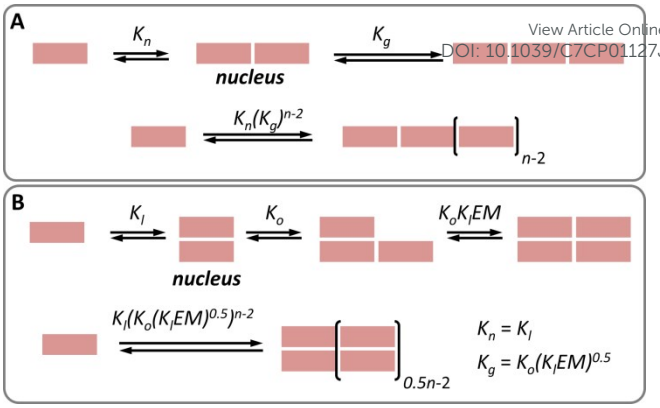


**Figure 4.**A. Schematic representation of the nucleation-growth of a single stranded polymer. B. Schematic representation of the nucleation-growth polymerization of a double stranded polymer showing the correspondence of the lateral and oligomerization constant in a double stranded polymer ($K_l$ and $K_o$) with the nucleation and growing constants ( $K_n$ and $K_g$) of general models of supramolecular polymerisation.

To understand why our system behaves differently, it is useful to direct our attention to the different ways polymers assemble and how cooperativity is defined. Typically, models of cooperative supramolecular polymerization assume that the formation of the initial nucleus is characterized by the nucleation constant $K_n$, and the growth of the polymer by the growth constant $K_g$ (Figure 4A). The cooperativity is often measured by the cooperativity factor $\alpha$, which is the ratio between $K_g$ and $K_n$:[22]

$$\alpha = \frac{K_g}{K_n} \qquad (8)$$

We have described the assembly of our double stranded polymer as the combination of two pairwise binding events, the lateral assembly and linear assembly, characterized by constants $K_l$ and $K_o$. The assembly process of the double stranded polymer can be seen as the dimerization of growing single stranded chains (Figure 1B). Alternatively, and for better comparison with traditional nucleation-growth models, it can be thought of as the polymerization of laterally assembled dimers (Figure 4B). In this scenario, the formation of the first lateral dimer is equivalent to the nucleation step in the nucleation growth of the double stranded polymers, and depends only on $K_l$. Subsequent polymerization steps depend on both $K_l$, $K_o$ and the effective molarity $EM$ (Figure 4B). For a building block that polymerizes following this mechanism the cooperativity factor $\alpha$ can be written as:

$$\alpha = \frac{K_o(EM)^{1/2}}{(K_l)^{1/2}} \qquad (9)$$

In the work of Schaefer *et al.*, involving a single stranded polymer, the calculations show that increasing salt concentration does have the effect of increasing $K_g$ but not $K_n$, leading to the corresponding increase in the cooperativity factor $\alpha$, according to equation (8). In our system, increasing the salt concentration has no effect on $K_o$, but increases $K_l$ which, according to equation (9) decreases the cooperativity factor. Therefore increasing $K_l$ leads to two somewhat

View Article Online
DOI: 10.1039/C7CP01127J



contrasting effects: one is the increase in overall stability of the polymer, and the second is the decrease in cooperativity (as predicted by eq.(9)) and because $K_o$ is constant since it is independent of the salt concentration. Clearly, our model shows that the interplay between the lateral association and the polymerization is critical in the degree of cooperativity observed. Our model can be expanded to the analysis of multistranded polymers with any number of strands. A convenient way to compare the degree of cooperativity in supramolecular polymerization is to plot the increase of concentration of monomer within the multi-stranded polymer **P** with addition of monomer **M**, $\Delta[\mathbf{P}]/\Delta[\mathbf{M}]_0$ *vs*. the total concentration normalized, that is, expressed in multiples of the maximum concentration of free monomer, $n[\mathbf{M}]_{max}$ (see Supplementary Information for details).

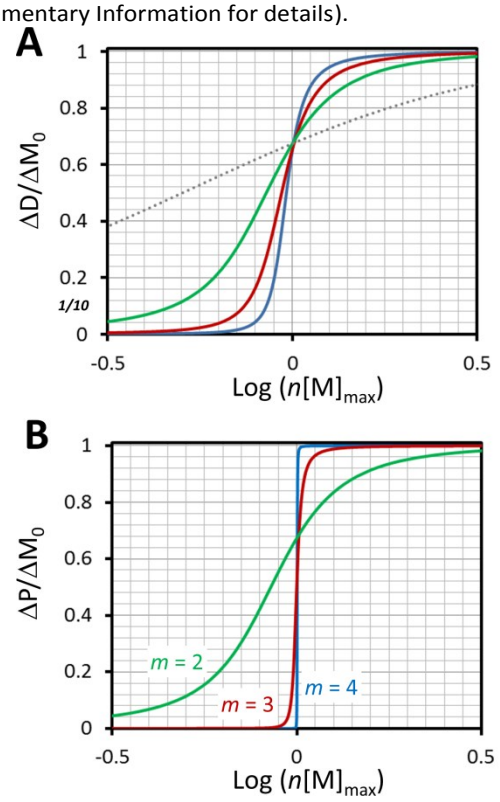


**Figure 5.** A. Cooperativity curves for double stranded polymers with values of $K_iEM$ = 5 blue trace), 500 (red trace) and 50000 (green trace). $K_o$ is 8400 $M^{-1}$ in all cases. B Cooperativity curves for multistranded polymers. The number of strands *m* is shown near the corresponding trace. $K_iEM$ is 50000 $M^{-1}$ and $K_o$ = 8400 $M^{-1}$. See Supplementary Figure 3 for traditional cooperativity plots for the same systems.

Larger cooperativity results in sharper curves, consistent with a sharper transition from quantitative assembly of discrete species to quantitative assembly of polymers. The increase in cooperativity as $K_i$ decreases is clearly seen for our double stranded polymer (Figure 5A). Strikingly, simulations for polymers with the same $K_o$ and $K_i$ values, but composed of more than two strands show a very large increase in cooperativity as the number of strands *m* increases (Figure 5B). This increase in the cooperativity with *m* is attributed to the fact that as the number of strands increases, so does the minimum size of the nucleus, which is composed of *m* building blocks. The larger the nucleus, the narrower the thermodynamic bottleneck that leads to the growth of the polymer, which leads to a larger cooperativity.

A clear dependence with the size of the nucleus is also observed with the traditional model of supramolecular polymerization, typically used for the assembly of single stranded and helical polymers (see Supplementary Information for details).[22] From our simulations, it is clear that, in systems where the nucleus contains more than 2 building blocks, the use of the parameter $\alpha$ as measure of cooperativity underestimates the cooperativity effect (Figure 6, Table 1). To compare cooperativity between systems with different sized nuclei we introduce the parameter $\alpha_m$, defined as follows:

$$\alpha_m = \left(\frac{K_g}{K_n}\right)^{m-1} \qquad (10)$$

where *m* is the number of building blocks in the nucleus, or the number of strands in a multi-stranded polymer. As shown in our simulations, $\alpha_m$ offers a good quantification of the cooperative behaviour for systems that display a clear cooperative effect (i.e., $\alpha \geq 10$). From these plots is also clear that very weak pairwise interactions may lead to very sharp cooperative behaviour for multistranded polymers with more than 5 strands (Figure 6, Table 1).

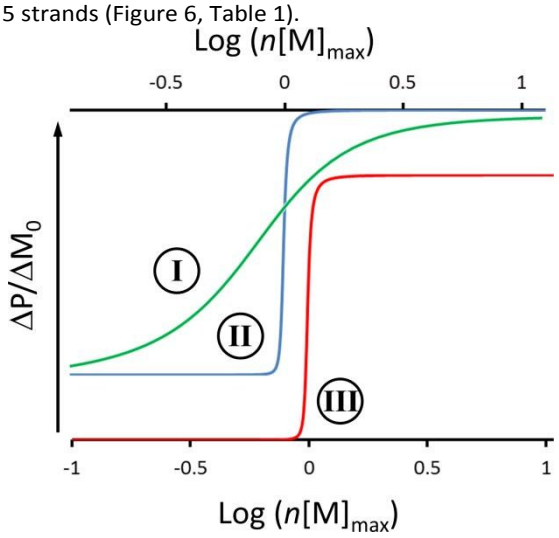


**Figure 6.** Cooperativity curves for polymer with 2 strands (or a nucleus containing 2 building blocks, traces I and II, x-axis labels shown in the top) and 6 strands (or a nucleus containing 6 building blocks, trace III, x-axis labels shown at the bottom). See Table 1 for detailed parameters used in these simulations.

**Table 1.** Parameters used to generate the curves displayed in Figure 6

| Curve | *m* | $K_n$ ($M^{-1}$) | $K_g$ ($M^{-1}$) | $\alpha$ | $\alpha_m$ |
|---|---|---|---|---|---|
| I | 2 | 10 | 100 | 10 | 10 |
| II | 2 | 10 | $10^6$ | $10^5$ | $10^5$ |
| III | 6 | 10 | 100 | 10 | $10^5$ |

## Conclusions

We have shown that our double stranded polymer assembles cooperatively following both changes in concentration of the building blocks and of salt. The cooperativity is explained in terms of a multivalence effect, for the dependence with the concentration of the building blocks, and in terms of an allosteric cooperative binding of countercations to the polymer, for the dependence with the concentration of salt. The net effect of the binding of the countercation is the increase of the lateral association constant, $K_l$. This increase in $K_l$ results in a decreasing *NC*, showing an increase in the stability of the polymer, but also to a less pronounced jump in polymer length upon nucleation, which suggest a lesser degree of polymerization cooperativity. This observation is the opposite of that found in other polymers, where the increase in stability induced by an increase in salt content results also in a more marked cooperativity. The difference in behaviour is attributed to the fact that, in our system, an increase in $K_l$ enhances nucleation to a larger extent than it enhances the growth. As a result, the cooperativity factor is smaller as $K_l$ increases. It has to be noted that the behaviour of our double-stranded polymer is caused by the fact that the countercations binding favour the dimerization more than the growth of the individual strands. Whether or not this effect is at play on the assembly of a double stranded polymer depends therefore on the specific chemical structure of the monomers. To graphically show the cooperativity effect, we propose using plots of the relative growth of the concentration of polymer with total concentration of monomer. These plots clearly show the relatively mild dependence of the cooperativity with $K_l$. Plots simulated for polymers with any number of strands show that cooperativity increases sharply as the number of strands increases. We attribute this effect to the increased size of the nucleus required, and we show that the there is a general strong dependence of the cooperativity with the size of the nucleus for any type of polymer. We propose the use of $\alpha_m$ as the parameter that allow comparing cooperativity for polymers with nuclei of any size

These findings clearly show that an ideal on/off polymerization does not require large pairwise interaction parameters between the building blocks, often difficult to achieve using small molecules. It suffices that the building blocks are designed to assemble into a polymer composed of 5 or more strands. Using this strategy will simplify the design and synthesis of highly responsive supramolecular polymers with improved properties for nanofabrication, controlled drug delivery and the assembly of bio-mimetic molecular machinery. Research in our labs is now directed to the development of highly responsive tri- and tetra-stranded porphyrin-based supramolecular polymers as sensor elements and for nanofabrication.

## Experimental

**Materials and methods**

Chemicals and solvents (including bipyridine **B**) where obtained from commercial sources and used without further purification. Cobalt porphyrin **C** was synthesized using a method described elsewhere.[34]

**UV titration-dilution experiments**

A stock solution containing **C** and **B** 109 mM in buffer phosphate 500 mM, pH 7.2, was prepared and serially diluted with a second solution containing the same concentration of **C** and **B** in pure water, to generate 9 stocks 109 mM in **C** and **B** but with buffer concentration ranging from 500 mM down to 2 mM. Each of these stocks was serially diluted with the corresponding buffer, so for each salt concentration, 9 samples were generated with the concentration of **C** and **B** ranging from 109 mM down to 0.43 mM. The samples were stored in stoppered plastic UV cuvettes at r. t. and kept in the dark. Their UV spectrum was recorded using a Cary300 UV spectrophotometer after equilibration overnight and again after one week. All the solutions prepared contained a 10% of $D_2O$, so that the samples could be used for NMR analysis.

**HPLC-SEC**

Size exclusion experiments were performed on selected samples, using an Agilent 1100 instrument equipped with a TSK-GEL G6000PW , 7.5mm x 30.0 cm column. The eluent was the buffer of the corresponding sample containing 2% of SDS to minimize non-ideal size exclusion behaviour due to absorption of the sample on the stationary phase. The injection volume for each of the samples was adjusted so that the same number of moles of C and B was injected (i.e., 0.1 nmol, corresponding to an injection of 100 uL for a concentration 1 uM in the sample, to 1 uL 100 uM. The UV detector was set at 430 nm, were all the species (monomer, small assemblies and polymers) absorb.

**NMR experiments**

The $^1$H NMR spectra of selected samples was performed using a Bruker AV600 NMR spectrometer.

## Acknowledgements

The authors will like to thank the Faculty of Science, Birkbeck, University of London, and Queen Mary University of London, for funding.

## Notes and references

1 T. F. A. De Greef, M. M. J. Smulders, M. Wolffs, A. P. H. J. Schenning, R. P. Sijbesma and E. W. Meijer, *Chem. Rev*., 2009, **109**, 5687.
2 T. Aida, S. I. Stupp and E. W. Meijer, *Science* 2012, **335**. 813.
3 J. D. Fox and S. J. Rowan, *Macromolecules*, 2009, **42**, 6823.
4 R. J. Wojtecki, M. A. Meador and S. J. Rowan, *Nat. Mater.*, 2011, **10**, 14.
5 X. Yan, F. Wang, B. Zheng and F. Huang, *Chem. Soc. Rev.*, 2012, **41**, 6042.
6 D. A. Fetcher and R. D. Mullinds, *Nature*, 2010, **463**, 285.
7 M, K. Gardner, B. D. Charlebois, I. M. Jánosi, J. Howard, A. J. Hunt and D. J. Odde, *Cell,* 2011, **146**, 582.
8 E. D. Korn, *Physiol. Rev*., 1982, **62**, 672.

View Article Online
DOI: 10.1039/C7CP01127J


9 L. Milanesi, C. A. Hunter, N. Tzokova, J. P. Waltho and S. Tomas, *Chem. Eur. J*., 2011, **17**, 9753.
10 E. A. Appel, J. del Barrio, X. J. Loh and O. A. Scherman, *Chem. Soc. Rev.*, 2012, **41**, 6195.
11 E. J. Howe, B. O. Okesola and D. K. Smith, *Chem. Commun*., 2015, 7451.
12 J. Zhang, and P. X. Ma, *Adv. Drug Deliv. Rev*., 2013, **65**, 1215.
13 J. Boekhoven and S. I. Stupp, *Adv. Mater.*, 2014, **26**, 1642.
14 R. N. Shah, N. A. Shah, M. M. D. Lim, C. Hsieh, G. Nuber and S. I. Stupp, *Proc. Nat. Acad. Sci. USA* 2010, **107**, 3293.
15 A. R. Hirst, B. Escuder, J. F. Miravet and D. K. Smith, *Angew. Chem. Int. Ed.*, 2008, **47**, 8002.
16 H. L.Anderson, *Chem. Commun.* 1999, 2323.
17 M.-H. M. Cativo, D. K. Kim, R. A. Riggleman, K. G. Yager, S. S. Nonnenmann, H. Chao, D. A. Bonnell, C. T. Black, C. R. Kagan and S.-J. Park, *ACS Nano*, 2014, **8**, 12755.
18 M. Gilbert and B. Albinsson, *Chem. Soc. Rev.*, 2015, **44**, 845.
19 R. Daly, O. Kotova, M. Boese, T. Gunnlaugsson and J. J. Boland, *ACS Nano*, 2103, **7**, 4838.
20 J. Leckie, A. Hope, M. Hughes, S. Debnath, S. Fleming, A. W. Wark, R.V. Ulijn and M. D. Haw, *ACS Nano*, 2014, **8**, 9580.
21 R. B. Martin, *Chem. Rev.*, 1996, **96**, 3043.
22 C. A. Hunter and H. L. Anderson, *Angew. Chem. Int. Ed.*, 2009, **48**, 7488.
23 D. H. Zhao and J. S. Moore, *Org. Biol. Chem.*, 2003, **1**, 3471.
24 L. H. Beun, X. J. Beaudoux, J. M. Kleijn, F. A. de Wolf and M. A. Stuart, *ACS Nano*, 2012, **6**, 133.
25 X. Ma and H. Tian, *Acc. Chem. Res.*, 2014, **47**, 1971.
26 C. Schaefer, I. K. Voets, A. R. A. Palmans, E. W. Meijer, P. van der Schoot and P. Besenius, *ACS Macro Lett*., 2012, **1**, 830.
27 Y. Tian, C. M. Beavers, T. Busani, K. E. Martin, J. L. Jacobsen, B. Q. Mercado, B. S. Swartzentruber, F. van Swol, C. F. Medforth and J. A. Shelnutt, *Nanoscale*, 2012, **4**, 1695
28 C. A. Hunter and S. Tomas, *J. Am. Chem. Soc*., 2006, **128**, 8975.
29 F. G. J. Odille, S. Jonsson, S. Stjernqvist, T. Ryden and K. Warnmark, *Chem. Eur. J.,* 2007, ***13***, 9617.
30 S. Ogi, K. Sugiyasu, S. Manna, S. Samitsu and M. Takeuchi, *Nature Chem*., 2014, **6**, 188.
31 E. Lopez-Fontal, L. Milanesi and S. Tomas, *Chem. Sci.* 2016, **7**, 4468.
32 A. Fidalgo-Marijuan, G. Barandika, B. Baza, M.-K. Urtiaga and M. I. Arriortua, *CrystEngComm*, 2013, **15**, 4181.
33 G. Scheiner-Bobis, *Eur. J. Biochem*., 2002, **269**, 2424.
34 M. Bhatti, T. D. McHugh, L. Milanesi and S. Tomas, *Chem. Commun.*, 2014, 7649.